Characterization of Natural and Affected Environments

Identification of Phosphorus Sources in a Watershed Using a Phosphate Oxygen Isoscape Approach

Takuya Ishida, Yoshitoshi Uehara, Tomoya Iwata, Abigail P. Cid-Andres, Satoshi Asano, Tohru Ikeya, Ken'ichi Osaka, Jun'ichiro Ide, Osbert Leo A. Privaldos, Irisse Bianca B. De Jesus, Elfritzson M. Peralta, Ellis Mika C. Triño, Chia-Ying Ko, Adina Paytan, Ichiro Tayasu, and Noboru Okuda

Environ. Sci. Technol., **Just Accepted Manuscript** • DOI: 10.1021/acs.est.8b05837 • Publication Date (Web): 02 Apr 2019

Identification of Phosphorus Sources in a Watershed Using a Phosphate Oxygen Isoscape Approach

Takuya Ishida,[1] Yoshitoshi Uehara,[1] Tomoya Iwata,[2] Abigail P. Cid-Andres,[3] Satoshi Asano,[4] Tohru Ikeya,[1] Ken'ichi Osaka,[5] Jun'ichiro Ide,[6] Osbert Leo A. Privaldos,[7] Irisse Bianca B. De Jesus,[8] Elfritzson M. Peralta,[8] Ellis Mika C. Triño,[8] Chia-Ying Ko,[9] Adina Paytan,[10] Ichiro Tayasu,[1] Noboru Okuda[1]*

[1]Research Institute for Humanity and Nature, 457-4, Motoyama, Kamigamo, Kyoto, 603-8047, Japan

[2]Faculty of Life and Environmental Science, University of Yamanashi, 4-4-37, Takeda, Kofu, Yamanashi 400-8510, Japan

[3]Department of Physical Sciences, College of Science, Polytechnic University of the Philippines, Anonas Street. Sta. Mesa, Manila, 1016, Philippines

16 [4]Lake Biwa Environment Research Institute 5-34, Yanagasaki, Ohtsu, Shiga, 520-0022,
17 Japan

18 [5]School of Environmental Sciences, The University of Shiga Prefecture, 2500, Hasaka,
19 Hikone, Shiga, 522-8533, Japan

20 [6]Institute of Decision Science for a Sustainable Society, Kyushu University, 394, Tsubakuro,
21 Sasaguri, Fukuoka, 811-2415, Japan

22 [7]Laguna Lake Development Authority, National Ecology Center, East Avenue, Diliman,
23 Quezon City, 1101, Philippines

24 [8]The Graduate School, University of Santo Tomas, España Boulevard, Manila, 1015,
25 Philippines

26 [9]Institute of Fisheries Science & Department of Life Science, National Taiwan University,
27 No. 1, Sec. 4, Roosevelt Rd., Taipei 10617, Taiwan

28 [10]Institute of Marine Sciences University of California Santa Cruz, 1156, High Street, Santa
29 Cruz, CA, 95064, USA

30

Corresponding Author

Takuya Ishida

tishida@chikyu.ac.jp

+81-75-707-2285

ABSTRACT. Identifying non-point phosphorus (P) sources in a watershed is essential for addressing cultural eutrophication and for proposing best-management solutions. The oxygen isotope ratio of phosphate ($\delta^{18}O_{PO4}$) can shed light on P sources and P cycling in ecosystems. This is the first assessment of the $\delta^{18}O_{PO4}$ distribution in a whole catchment, namely the Yasu River Watershed in Japan. The observed $\delta^{18}O_{PO4}$ values in the river water varied spatially from 10.3‰–17.6‰. To identify P sources in the watershed, we used an isoscape approach involving a multiple-linear-regression model based on land use and lithological types. We constructed two isoscape models, one using data only from the whole watershed and the other using data from the small tributaries. The model results explain 69% and 96% of the spatial variation in the river water $\delta^{18}O_{PO4}$. The lower R^2 value for the whole watershed model is attributed to the relatively large travel time for P in the main stream of the lower catchment that can result in cumulatively biological P recycling. Isoscape maps and a correlation analysis reveal the relative importance of P loading from paddy fields and bedrock. This work demonstrates the utility of $\delta^{18}O_{PO4}$ isoscape models for assessing non-point P sources in watershed ecosystems.

1.0. INTRODUCTION

Anthropogenic phosphorous (P) loads have increased in many watersheds because of industrialization and urbanization, resulting in serious cultural eutrophication issues in aquatic ecosystems. To mitigate such cultural eutrophication, watershed management has been practiced to reduce P loads from point sources through institutional and technological approaches, including (i) laws to regulate nutrient loadings and (ii) installing wastewater treatment plants (WWTPs).[1–3] Nevertheless, compared to point sources, it has been more difficult to regulate non-point P sources (e.g., anthropogenic loads from agricultural and urban activities, natural loads from forests and bedrocks, and atmospheric deposition[4]) primarily because it is difficult to assess the contribution of each non-point source to the total load. Therefore, to overcome this limitation related to P pollution, apportioning point and non-point sources and long-term assessment of these contributions are important.[3,5,6]

Studies are increasingly using the oxygen isotope ratio of phosphate ($\delta^{18}O_{PO4}$) to understand P dynamics in both aquatic and terrestrial ecosystems,[7–10] and reference therein. Because the P–O bonds in phosphate do not easily hydrolyze at typical earth's surface temperatures and pressures, $\delta^{18}O_{PO4}$ values in environmental samples are imprinted with the isotopic signatures of the P sources provided P uptake and utilization by organisms is limited.[7,9] Biological processes mediated by enzymes that cleave the P–O bonds cause large isotopic fractionation.[11–

[15] For example, intracellular activity of inorganic pyrophosphatase (PPase) can alter the isotopic signatures of environmental phosphate samples and appears to dominate the $\delta^{18}O_{PO4}$ signature of inorganic phosphate (Pi) pool in most natural aquatic systems.[7,16] The $\delta^{18}O_{PO4}$ of the Pi pool that has been catalyzed by PPase reaches temperature-dependent isotope equilibrium on relatively short time scales, and several equations have been proposed to estimate the equilibrium value.[14,15] Those equations can be used to estimate the biological recycling of P in ecosystems based on the extent to which source isotope signatures are overwritten by such biological processes and are approaching the equilibrium value.[7]

$\delta^{18}O_{PO4}$ has not been used much in freshwater systems, such as rivers and lakes, primarily because of inorganic and/or organic compounds in these freshwater samples that interfere with the precipitation of phosphate as pure silver phosphate used for isotope analysis.[9] This problem can be overcome partially by adding more purification steps[9]; however, using the $\delta^{18}O_{PO4}$ system remains challenging for systems with low dissolved Pi concentration and high concentration of dissolved organic matter.[17,18] Despite these difficulties, P sources can be identified using $\delta^{18}O_{PO4}$ in subcatchments with measurable P loads.[6,17–21] To identify non-point P sources from natural and anthropogenic loading in a watershed, it is important to determine the sources of P from head catchments that can be sensitive to human disturbance because of

84 their small water volume[22] to the downstream catchments that are typically influenced by
85 multiple P sources.
86 In the present study, we conducted synoptic sampling of river water and potential P sources
87 in the whole catchment of the Yasu River, a tributary of Lake Biwa in Japan [Fig. 1(a)] to
88 identify natural and anthropogenic P sources, especially non-point sources, using $\delta^{18}O_{PO4}$.
89 Although isotope mixing models have been used previously to quantify the relative
90 contribution of P sources in simple and small-scale systems with only a few P sources,[21,23] this
91 approach has yet to yield realistic solutions in complex watershed systems. Here, we use a
92 $\delta^{18}O_{PO4}$ isoscape (isotopic landscape) approach to assess P sources throughout the entire
93 catchment of the Yasu River. The isoscape approach allows us to visualize the contribution of
94 sources and biogeochemical processes and to link the spatial pattern of river water $\delta^{18}O_{PO4}$
95 values to site characteristics such as land use and lithological type.[24–26]
96
97 2.0. MATERIALS AND METHODS
98 **2.1. Study Site.** Our study area encompasses the entire catchment of the Yasu River, the
99 largest tributary in Lake Biwa Watershed (LBW) in Japan [Fig. 1(a)]. Lake Biwa was
100 oligotrophic until the 1950s, but since then, cultural eutrophication due to rapid
101 industrialization and urbanization has been prevalent.[5] In 1979, Shiga Prefecture (governing

this watershed) imposed legislation to mitigate this cultural eutrophication. It then promoted the installation of wastewater treatment plants (WWTPs) to reduce nutrient loadings from industrial and domestic point sources. From the 1980s to the present, the total P load into the lake has been halved.[27]

The Yasu River originates from Mt. Gozaisyo, at 1,213 m elevation. Its river length and catchment area are 65.3 km and 387 km^2, respectively. Precipitation and temperature range from 1,618 mm and 15.5 °C in the lower (Ohtsu) catchment to 1,637 mm and 13.6°C in the upper (Tsuchiyama) catchment (annual means from 2007 to 2016). The catchment is covered by forest (55%), cropland (24%), and built-up (11%) land uses [Fig. 1(b)]. The dominant crop in the catchment is rice, occupying 91% of the cropland area. The irrigation period of rice paddies is typically from April to September. The Yasu River Watershed (YRW) is characterized by three lithological types: an accretionary complex (18%), granite (22%), and sedimentary rocks (59%) [Fig. 1(c)].

Domestic wastewater in this catchment is treated at one large WWTP as well as in many smaller-scale WWTPs. The large WWTP, located outside the catchment [Fig. 1(a)], services 91.4% of the human population in 5 local government areas overlapping YRW, and its effluent is discharged into the nearby lake basin not impacting the Yasu River.[27] The smaller WWTPs

119 are located in the rural areas of the upper catchment [Fig. 1(a)], and their effluents are
120 discharged directly into the nearby stream tributaries of the Yasu River.

121 **2.2. Sample Collection.** River water samples for $\delta^{18}O_{PO4}$ analysis were collected using a
122 plastic bucket and then emptied into 20 L polyethylene containers at 30 sites representing first-
123 to fifth-order streams whose catchments differ in land use and lithological type (Fig. 1). The
124 sampling sites were established upstream of river confluences to uniquely characterize
125 respective tributaries to the main stem. A synoptic survey was conducted in May 2016 at the
126 beginning of the paddy irrigation period. The sample volumes were 20–40 L depending on the
127 soluble reactive phosphate (SRP) concentration at each site, measured prior to sample
128 collection. River water samples were collected from shallow channel units (e.g. riffle, rapid, or
129 glide) in each sampling site where river waters are well mixed by turbulent flow.

130 Locations of the water sampling sites were selected to represent potential non-point source
131 end members in the watershed based on a specific land use, lithological distribution, and P
132 loads according to a report of Shiga Prefecture estimating the P loads into LBW using a
133 simulation model.[28] Potential sources that contribute dissolved Pi to the river/tributaries in the
134 catchment, composed of bedrocks, forest-floor soils, paddy soils, fertilizers, and WWTP
135 effluents, were also collected [Fig. 1(a) and Tables S1–S4]. In head catchments characterized
136 by a single rock type [sites 29 and 56 (IDs: R4 and R3) for granite and sites 70 and 201 (R1

and R2) for accretionary complex rocks], a riverbed gravel was collected as a representative of the lithology. This gravel is assumed to be a better representative of the rocks in the subcatchment than the bedrock because this sample integrates and encompasses the bedrock heterogeneity, if any exists. To remove organic matter attached to the riverbed gravel, the samples were sieved into 1–4.75 mm fraction and then rinsed thoroughly with ultra-pure water (UPW). To represent the sedimentary rocks in the basin, a sample (R5) was handpicked from a fault area in the sedimentary rock layer near site 44 (Fig. 1) because other rock exposures were not attainable. Forest soil samples were collected in the areas covered by the Japanese Cedar forests to represent sites with different bedrock types, thus possibly affecting the $\delta^{18}O_{PO4}$ value in soils.[29] The soil samples were collected from the A horizon (about 0–10 cm depth) at three points per site (S3–10; Fig. 1) and then combined as one sample. The samples of rice paddy soil were collected from the depth of about 10 cm corresponding to the upper root layer at the center of two different paddy fields (S1 and S2) in December 2015, which is a non-irrigation period to avoid crop damage. These rice paddies are owned by different famers, allowing us to examine differences in their farming practices on $\delta^{18}O_{PO4}$ value. The farmers also provided us with manufactured organic (F1) and chemical (F2) fertilizers commonly used in Shiga Prefecture. These organic and chemical fertilizers contain 8% and 28% P, respectively, as indicated by the manufacturer. The water-soluble Pi content of these fertilizers analyzed in

this study is presented in Table S4. We also obtained a stock solution (F3) of the manufactured chemical fertilizers from the company that supplies around 90% of the products distributed by the Japan Agricultural Cooperatives (JA) in Shiga Prefecture (JA, personal communication). WWTP effluent samples (5 L each) were collected with a plastic bucket directly from a final storage pool at six (W1–W6) of the small-scale WWTPs in the rural areas of the upper catchment [Fig. 1(a)] in August 2018, and kept in 10 L polyethylene containers until analysis.

To calculate the theoretical expected isotope equilibrium values of $\delta^{18}O_{PO4}$ of different samples, river water, WWTP effluent and paddy irrigation water samples were collected for water oxygen isotope ratios ($\delta^{18}O_{H2O}$). The water temperature in the river was measured using a logger (UA-002-64; Hobo) installed at each of the 30 sampling sites for more than three days to obtain the daily average. For the WWTP effluent samples, the water temperature was measured using a multiprobe (ProDSS; YSI Inc., USA). The temperature of the irrigation water was measured with the logger set at the three rice paddies in the catchment of site 44 during the irrigation period.

2.3. Sample Preparation. Water samples were filtered through 0.2-μm membrane filters (Advantec) for measurement of $\delta^{18}O_{H2O}$ and SRP concentration, and through 0.45-μm membrane filters (Advantec) for $\delta^{18}O_{PO4}$ analysis, within 24 hours from collection. Following

the filtration, $MgCl_2$ was added to the samples used for $\delta^{18}O_{PO4}$ analysis and the pH increased to ~10.5 to remove the phosphate as brucite (magnesium-induced co-precipitation, MAGIC).[30]

The rock and gravel samples were washed using UPW, dried at 50°C, and ground to powder using a multi-bead shocker (Yasui Kikai, Japan) with tungsten carbide beads to homogenize the samples and to enhance the reaction between extraction solution and the sample. The samples were stored at room temperature until analysis. The powdered samples were immersed in 1 M HCl for 16 h to extract the soluble Pi.[31] Soil samples were air dried and sieved through a 2-mm mesh and stored at room temperature until analysis (~1 year). Labile and weakly absorbed Pi in the soils was extracted with a 0.5 M $NaHCO_3$ solution.[31] The $NaHCO_3$ extractable Pi in our study may include microbial Pi, because soil drying lyses bacterial cells.[32] Although storing soil at room temperature without drying processes changes the $\delta^{18}O_{PO4}$ value of labile Pi (~3.6‰),[33] the changes in the $\delta^{18}O_{PO4}$ values of $NaHCO_3$ extractable Pi in our soil samples during storage should have been limited because of completely drying the samples. The organic and chemical fertilizers were dried at 50°C and powdered to extract their labile phosphate with the UPW.

2.4. Sample Analysis. The SRP concentration of each samples was measured using the molybdenum-blue method[34] on a microplate spectrophotometer (Multiskan GO; Thermo Fisher Scientific). The detection limit of this devise is 0.08 μmol L^{-1} and the repeatability based

on duplicate analyses of the same samples (±SD) is ± 0.02 μmol L^{-1}. For the $\delta^{18}O_{PO4}$ analysis, inorganic phosphate samples were converted to Ag_3PO_4 according to McLaughlin et al.[30] with the addition of a solid-phase extraction step to remove dissolved organic matter (Fig. S1).[35]

The $\delta^{18}O_{PO4}$ values reported relative to the Vienna Standard Mean Ocean Water (VSMOW) of the Ag_3PO_4 samples were measured using a TC/EA-IRMS (thermal conversion elemental analyzer connected to a Delta plus XP via ConFlo III, Thermo Fisher Scientific) at the Research Institute for Humanity and Nature (RIHN). Three internal standards with values of 8.3 ± 0.29‰, 14.4 ± 0.14‰, and 23.1 ± 0.27‰ were used for calibration and normalization after calibration with two independently calibrated standards (STDL: 11.3 ± 0.15‰; STDH: 20.0 ± 0.25‰) reported by McLaughlin et al.[30] The analytical precision (±SD) was ± 0.4‰. Three replicates of rock and soil samples were prepared for $\delta^{18}O_{PO4}$ analysis. The standard deviation of the triplicate measurements was less than 0.5‰, demonstrating the reliability and reproducibility of the method.

$\delta^{18}O_{H2O}$ values were measured using a water isotope analyzer (L2120-I; Picarro, USA) with an analytical precision of 0.05‰. The expected equilibrium values ($\delta^{18}O_{PO4\ Eq}$) were estimated using the following empirical equation:[14]

$$\delta^{18}O_{PO4\ Eq} = \delta^{18}O_{H2O} - (T + 273.15)/4.3 + 25.9, \quad (1)$$

where $\delta^{18}O_{H2O}$ is the oxygen isotope ratio (‰) of ambient water and T [K] is the water temperature.

2.5. Isoscape Approach. Land cover and lithological type in the watershed were determined for each sampling site using a geographic information system (ArcGIS 10.2; ESRI Japan). We used a 1/50,000 digitized vegetation map obtained from the Biodiversity Center of Japan to determine the areal proportion of four land-cover types (forest, paddy field, built-up, other) for the catchment of each sampling site. We also used a 1/200,000 digital geological map published by the Geological Survey of Japan to calculate the proportional area of each lithological type (accretionary complex, granite, sedimentary rock) for each catchment.

To delineate the $\delta^{18}O_{PO4}$ isoscapes of the entire river system, we used a multiple regression analysis incorporating as explanatory variables the proportional areas of the land cover (forest, paddy field, and built-up) and lithological types (accretionary complex, granite, and sedimentary rock) that are deemed to be potential non-point P sources in the YRW. We constructed two models: (i) a watershed model and (ii) a tributary model, based on the $\delta^{18}O_{PO4}$ values of (i) all sampling points of the entire watershed and (ii) those located in tributaries with catchment areas of less than 20 km^2, respectively (Table S1). In the tributary model, the $\delta^{18}O_{PO4}$ level is likely determined primarily by the source isotopic signatures because of the short P transport distance (travel time) and hindering biological P uptake due to the relatively

low light intensity in forest streams[6,36] of our study area, although the biological uptake differs on the basis of the headwater characteristics, such as relative benthic area to water volume and connectivity with the riparian and hyporheic zones.[22] In the watershed model, by contrast, we expect the $\delta^{18}O_{PO4}$ values to be modified by the cumulative effects of metabolic processes due to a longer travel time for P along the river course. For each of these two models, the best fit was selected from all possible combinations of the explanatory variables based on Akaike's Information Criterion (AIC) to minimize the information and variance inflation factor (VIF) to avoid multicollinearity (criterion: VIF < 10). The statistical analyses were conducted using R version 3.4.4.[37]

Prior to isoscape mapping, 489 points including the actual sampling points were set along the river on the GIS map, whereupon the watershed characteristics of land cover and lithological type were analyzed for each point as mentioned above. The $\delta^{18}O_{PO4}$ value at each point was predicted using the best fits for the watershed and tributary models. To project the isoscape maps, we interpolated the predicted values of $\delta^{18}O_{PO4}$ spatially for the entire river system using the inverse distance weighting (IDW) tool of ArcGIS to take the inverse-distance-weighted average between neighborhood points.

3.0. RESULTS AND DISCUSSION

3.1 $\delta^{18}O_{PO4}$ Values in River Water. Although we collected river water from 30 sites in the Yasu River, we obtained a sufficient amount of Ag_3PO_4 for $\delta^{18}O_{PO4}$ analysis from only half the samples ($N = 15$). This may be attributed to the very low orthophosphate concentrations in the samples that did not yield sufficient Ag_3PO_4. Prior to our synoptic sampling, we calculated the water volume needed for $\delta^{18}O_{PO4}$ analysis based on a preliminary survey of the SRP concentrations at each site. Nevertheless, this estimate was higher than the Pi in the samples; it is known that SRP measured by the molybdenum-blue method includes P species other than orthophosphate,[38] explaining this overestimation. Recently, Maruo et al.[39] reported that the ratio of orthophosphate to SRP in river and lake water samples collected from the Lake Biwa Watershed (LBW) varied widely from 0.06 to 0.79, requiring more than 10 times the volume of water we collected to obtain enough Ag_3PO_4. Accordingly, it is recommended that water samples of volume much larger than needed be collected for the $\delta^{18}O_{PO4}$ analysis,[7] assuming that the freshwater samples have a low orthophosphate-to-SRP ratio.

Within the Yasu River Watershed (YRW), the $\delta^{18}O_{PO4}$ values of dissolved Pi in river water that could be measured ranged from 10.3‰ to 17.6‰ (Fig. 2). Similarly large variations have been observed in other coastal and freshwater systems,[9] in which P sources and P metabolic processes are expected to have high spatiotemporal variability. For example, the $\delta^{18}O_{PO4}$ values dissolved Pi in watersheds around Lake Erie span 4.7‰, in the San Joaquin River System

7.2‰, and in the Lake Tahoe watershed 3.0‰.[40] By contrast, in the catchment of the River Taw in southwest England, the $\delta^{18}O_{PO4}$ values of dissolved Pi in river water vary by only 1.7‰ along the main channel from upstream to downstream sites.[17] The $\delta^{18}O_{PO4}$ values for the water in the River Taw catchment are similar to those expected from theoretical equilibrium at all sites and differ from those of potential natural and anthropogenic P sources, suggesting that in this river the source isotope signatures are overwritten by in-stream biological processes.

In the YRW, the $\delta^{18}O_{PO4}$ values of dissolved Pi deviate greatly from the $\delta^{18}O_{PO4\ Eq}$ for many tributary streams (Fig. S2), indicating that phosphate ions in the river water are not being taken up fully by the living biomass in the streams and these values can be utilized for identifying P source in the watershed. The rate of biological P recycling depends on stream characteristics such as biological activity, nutrient balance and travel time.[6,17,19,41] We surmise the relatively small catchment area (387 km^2), steep gradient (87–1,213 m in elevation) and high flow velocity (0.79 ± 0.62 km/h; Table S1) of the Yasu River may result in a travel time that is too short for complete in-stream microbial P turnover.[6,36] Consequently, the Yasu River has a wide range of $\delta^{18}O_{PO4}$ values imprinted by isotope signatures derived from various P sources that dominate different sections of the watershed.

3.2. $\delta^{18}O_{PO4}$ Values in Natural and Anthropogenic P Sources. Our source samples have distinct $\delta^{18}O_{PO4}$ values (Fig. 2), allowing us to examine the relative importance of each source

to the river. According to the previous studies, $\delta^{18}O_{PO4}$ values in source samples vary widely that cover all the range of our source sample (details are shown in below). [7–10]

3.2.1. Bedrocks and forest-floor soils. The $\delta^{18}O_{PO4}$ values of HCl extractable Pi in bedrocks differs based on rock types (Fig. 2 and Table S4). The granite rocks (R3 and R4) found in the upstream mountain area and within the watershed of some of the first-order streams in the lower catchment (Fig. 1) have the $\delta^{18}O_{PO4}$ value range of 11.4–13.4‰ whereas sedimentary rock values is 18.5‰ (R5) (Fig. 2 and Table S4). The extracted bedrock Pi using 1M HCl mainly constitutes the calcium-bound P fraction (e.g., apatite).[31] Apatite in plutonic rocks generally has low $\delta^{18}O_{PO4}$ values (6.0–13.5‰),[42–44] which are similar to the granite $\delta^{18}O_{PO4}$ values observed in the YRW. By contrast, because $\delta^{18}O_{PO4}$ values in biotic apatite are determined from the $\delta^{18}O_{H2O}$ values of ambient water and the temperature during apatite formation, sedimentary apatite shows great variation with rock age and location (6.0–25.0‰).[14,45] Our sedimentary rock value is consistent with those of biotic apatite. The accretionary complex comprises a mixture of igneous and biotic apatite, and thus the $\delta^{18}O_{PO4}$ values of HCl extractable Pi in the accretionary complex (11.0–11.1‰) are controlled by the relative contribution of these rock types.

In the present study, we were unable to characterize the $\delta^{18}O_{PO4}$ values of $NaHCO_3$ extractable Pi in the forest-floor soils. Japanese forest soils typically have low labile Pi

297 concentrations (Table S4) and high organic-matter content,[46] preventing $\delta^{18}O_{PO4}$ analysis.[47,48]
298 According to the previous studies, the $\delta^{18}O_{PO4}$ values in soil samples vary between different
299 operationally defined soil fractions.[8,29,48–50] In natural systems, the $\delta^{18}O_{PO4}$ values of labile and
300 less labile P fractions are typically close to that expected at the isotopic equilibrium with water
301 and that of the parent rock material, respectively,[29,49,50] although this phenomenon is not always
302 the case and actual values also depend on pedogenesis processes, such as weathering rate and
303 biological activity.[51,52] If the former case (i.e. equilibrium) applies to our study area, then the
304 $\delta^{18}O_{PO4\ Eq}$ values of labile Pi in forest soils are estimated to be around 15.3‰ based on the
305 average $\delta^{18}O_{H2O}$ (−6.41‰) and the air temperature (18°C) in the upper catchment
306 (Tsuchiyama) during the sampling period. This value differs from that of $\delta^{18}O_{PO4,}$ which we
307 measured for accretionary complex and granite rock. Therefore, forest soil is possibly the
308 source with a wide value range of $\delta^{18}O_{PO4}$ to the river.

309 **3.2.2. Fertilizers and rice-paddy soils.** In our analysis, the $\delta^{18}O_{PO4}$ values of water soluble
310 P in chemical and organic fertilizers differ (Fig. 2 and Table S4), which may depend on raw
311 material of phosphate used to produce the fertilizer. Previous studies reported that
312 manufactured fertilizers show a wide range of $\delta^{18}O_{PO4}$ values (15.5–27.0‰), reflecting the
313 isotopic signatures of the phosphate ores used in production.[10,40,53] Our chemical-fertilizer
314 sample (F2, 12.7‰) had a $\delta^{18}O_{PO4}$ signature similar to that of its stock solution (F3, 13.1‰),

315 which is used for many manufactured products that have a large market share in Shiga
316 Prefecture. A value of 12–13‰ can therefore be regarded as representative isotopic signature
317 that is characteristic of chemical fertilizers in the YRW.

318 The $\delta^{18}O_{PO4}$ values of $NaHCO_3$ extractable Pi in rice-paddy soil samples collected at two
319 different places during the non-irrigation period had almost the same values (18.0–18.2‰)
320 (Fig. 2 and Table S4). These values may be controlled by fertilizer addition and/or biological
321 recycling. These values are similar to that of the organic fertilizer value (F1, 17.2‰), although
322 they differ from that of the chemical fertilizer (Fig. 2 and Table S4). One possibility is that the
323 organic fertilizer sets the $\delta^{18}O_{PO4}$ values of $NaHCO_3$ extractable Pi in the paddy soils. Another
324 explanation is that the biological recycling of labile Pi derived from fertilizers in rice paddies
325 determines the paddy soil signature. A previous study reported that the $\delta^{18}O_{PO4}$ values of labile
326 Pi in irrigated soils rapidly approach to an equilibrium value within half a month of adding P
327 fertilizers, thus overwriting the source isotope signatures.[54,55] Therefore, the $\delta^{18}O_{PO4}$ values of
328 $NaHCO_3$ extractable Pi in rice paddy soils may depend on the seasonality in water temperature
329 and $\delta^{18}O_{H2O}$. We estimated the equilibrium value expected in the sampling period based on our
330 monitoring data of $\delta^{18}O_{H2O}$ (-3.46 ± 1.05‰) and the water temperature (20.9 ± 4.8°C) of the
331 irrigated water in the rice paddies during sampling period. The resulting $\delta^{18}O_{PO4\ Eq}$ value is
332 17.6‰. If indeed Pi in rice paddies is almost completely recycled, then the observed $\delta^{18}O_{PO4}$

in river water was derived from rice paddy wastewater flowing to the river through agricultural drainage canals or culverts.

3.2.3. WWTP effluents. The $\delta^{18}O_{PO4}$ values of dissolved Pi in the wastewater treatment plant (WWTP) effluents are relatively constrained, spanning a narrow range (Fig. 2), suggesting that these isotopic signatures are typical of the WWTP effluents in this watershed. Effluents from WWTPs are often considered to be the primary point sources of domestic P in a river.[18,19] In the entire LBW, the point sources from the WWTPs account for 16.1% of the total P loading into the lake basin.[28] To estimate the contribution of the WWTP-derived P discharged into the tributaries of the Yasu River, we calculated the P load from each small-scale WWTP using the maximum discharge and SRP concentration of its effluent. The estimated P load ranged from 8.85 to 63.6 mmol/day, which is large enough to alter the $\delta^{18}O_{PO4}$ values of dissolved Pi in the river water in small tributaries (Table S2). However, even for a site in a small tributary (site 44) that is located immediately downstream from a small-scale WWTP [Fig. 1(a)], the $\delta^{18}O_{PO4}$ value of dissolved Pi in the river water (17.6‰) differs markedly from that in the WWTP effluent (14.0–15.9‰) (Tables S2 and S3). This result differs from reported conditions in the River Beult in the United Kingdom, in which the $\delta^{18}O_{PO4}$ values of dissolved Pi in the river downstream from a WWTP were found to be similar to those of the WWTP effluents.[18] In our case, intermittent discharge from WWTP may result in the difference

between the $\delta^{18}O_{PO4}$ value in WWTP effluent and downstream tributary water. Thus, the actual $\delta^{18}O_{PO4}$ values of dissolved Pi in the downstream tributary water should show large temporal variation depending on the discharge times and rates from the WWTPs.

Considering that the river discharge in the main stream is much greater than water volumes added by the small-scale WWTP effluent disposal, the WWTP-derived P may be diluted substantially with river water in the lower catchment. The fact that effluent from the large WWTP that serves more than 90% of the watershed population is not discharged directly into the Yasu River suggests that the impact of the WWTPs on the $\delta^{18}O_{PO4}$ values of dissolved Pi in the river water is not great overall.

3.3. $\delta^{18}O_{PO4}$ Isoscapes. The watershed and tributary models for $\delta^{18}O_{PO4}$ isoscapes account for 69% and 96% of the spatial variation in the $\delta^{18}O_{PO4}$ values dissolved Pi in the river water, respectively. These values are sufficiently high when constructing an isoscape map (Table 1).[31] The best-fit model of the $\delta^{18}O_{PO4}$ isoscapes is the one that uses the proportional areas of rice paddy, forest, and accretionary complex as explanatory variables to be employed as predictors for the watershed model and that of granite and same predictors of the watershed model for the tributary model. The isoscape maps of the $\delta^{18}O_{PO4}$ values of dissolved Pi in the river water, based on two models, exhibit a similar trend (Fig. 3), that is, low value in the upstream and average–high value in the middle and downstream.

Although the predicted values using the two models significantly correlated with each other (Pearson's $r = 0.73$; $p < 0.05$), the average and SD of the predicted values from the tributary model (13.6 ± 2.6‰) were significantly higher than that from the watershed model (12.8 ± 2.0‰) ($p < 0.05$; t test for average and F test for SD). The differences in averages, SDs, and R^2 values of the two models may be caused by isotope fractionation associated with microbial P turnover particularly in lower stream. Since small tributaries in the upper catchments are expected to have low microbial P turnover due to low forest canopy openness (0.36 ± 0.22, Table S1) and high flow velocity (Table S1),[6,36] the source isotope signatures are dominant in the Pi pool of these streams. Meanwhile, the main stream in the lower catchment has a long travel time for P in open water, thereby cumulatively enhancing the biological P recycling during its downward movement. These differences may affect model predictions and result in the lower R^2 value for the watershed model. Hence, future work will involve incorporating in-stream biological processes into the models to fully understand the P dynamics in the entire watershed.

Non-point agricultural loads have been regarded as a major P source (16.0%) similar to the contributions from WWTPs (16.1%) and septic tanks (15.5%) based on a simulation model for the annual total P loads from LBW watershed into Lake Biwa in 2015.[28] In addition, the P loads from rice paddies during the irrigation period (4.82 kgP ha^{-1} day^{-1}) was estimated to be 2.6

387 times higher than that in the non-irrigation period (1.86 kgP ha^{-1} day^{-1}).[28] Therefore, the P
388 loads from the rice paddies are expectedly the highest P source during irrigation period. Indeed,
389 in our study, the river reach with high $\delta^{18}O_{PO4}$ values corresponds to areas dominated by rice
390 paddies that are situated on sedimentary rocks (Figs. 1 and 3 and Table S5). Moreover, the
391 proportional area of rice paddies shows the strongest positive correlation with the river water
392 $\delta^{18}O_{PO4}$ among the land cover and lithological types (Figs. S3 and S4). In the rice paddies,
393 chemical fertilizer expected to be the major inorganic P source because of its use in high
394 concentrations and its lability (Table S4), however, the $\delta^{18}O_{PO4}$ value of the fertilizer phosphate
395 is much lower than that observed in stream water even where the proportional area of rice
396 paddies is high [Fig. S3(a)]. The $\delta^{18}O_{PO4}$ values of dissolved Pi in the river water are similar to
397 those of organic fertilizer, rice-paddy soils, and sedimentary rocks, which have similar
398 signatures. We suggest that in the rice paddies, most of the labile Pi from fertilizer application
399 is turned over during the irrigation period, effectively erasing the source signature, as discussed
400 in the section 3.2.2. Taken together, the P derived from sedimentary rock and biologically
401 recycled P are likely to be the dominant non-point P sources to the river water in areas adjacent
402 to the rice-paddies.

403 Because the forest streams in our study area have few anthropogenic P sources (and low SRP
404 concentrations), we expect natural P sources such as bedrocks and forest soils to make a

relatively large contribution in forest streams. Indeed, the isoscapes show low $\delta^{18}O_{PO4}$ values of dissolved Pi in the upstream reaches of the river, where forest developed on accretionary complex and granite bedrock is abundant (Figs. 1 and 3 and Table S5). The proportional area of forest is not correlated significantly with the $\delta^{18}O_{PO4}$ value of dissolved Pi in river water (Fig. S3c); instead, the $\delta^{18}O_{PO4}$ values show a tendency to converge to that of granite and accretionary complex bedrock. This result indicates that bedrock and/or P pools in forest soils, with $\delta^{18}O_{PO4}$ value reflecting that of bedrocks,[29,49,50] are the dominant P sources in the forested areas.

We successfully demonstrated that the $\delta^{18}O_{PO4}$ isoscape models are promising tools for assessing non-point sources of anthropogenic and natural P loadings into a watershed because potential sources, such as land cover and lithological type had distinct $\delta^{18}O_{PO4}$ values. However, we also had a limitation on the precision of the estimation in a watershed scale because the isoscapes herein are based on a small dataset of $\delta^{18}O_{PO4}$ values. Therefore, in future studies, obtaining additional $\delta^{18}O_{PO4}$ data of river water and P sources is important to improve the model. We also need to consider and include additional factors affecting the $\delta^{18}O_{PO4}$ value in river water, such as existence of additional P sources (e.g., bank erosion, atmospheric deposition, internal loads from river sediment, and seasonal change in P loads from each P source). In addition, complementing the isoscape models by using other independent methods,

423 such as synoptic monitoring and hydrological models, is probably necessary. The isoscape
424 approach should be applicable in watersheds with similar characteristics to that of our
425 watershed and useful for watershed management, wherein excellent practices are designed to
426 reduce the P loads to control cultural eutrophication in river and lake ecosystems.
427
428

429 ACKNOWLEDGMENTS

430 This research was supported by the RIHN Project (grant no. D06-14200119) and the River
431 Foundation (grant nos. 28-5211-047 and 261211010). The sampling of the riverbed rocks was
432 conducted with permission of the Kinki Regional Development Bureau Office, Ministry of
433 Land, Infrastructure, Transport & Tourism. The public sewage division of Koka City and Yasu
434 City provided monitoring data on the small-scale WWTPs and logistic support to sample their
435 effluents. The Central Glass Co., Ltd provided the stock solution of the manufactured chemical
436 fertilizers. We thank to T. Ohta, T. Haraguchi, and R. Shibata for their technical advice on data
437 analysis.
438

439 ABBREVIATIONS

AIC, Akaike's Information Criterion; IDW, Inverse distance weighting; IRMS, Isotope-ratio mass-spectrometer; JA, Japan Agricultural Cooperatives; LBW, Lake Biwa Watershed; P, Phosphorus; Pi, Inorganic phosphate; RIHN, Research Institute for Humanity and Nature; SRP, Soluble reactive phosphate; UPW, Ultra-pure water; VIF, Variance inflation factor; YRW, Yasu River Watershed; VSMOW, Vienna Standard Mean Ocean Water; Yasu River Watershed; WWTP, Wastewater treatment plant

SUPPORTING INFORMATION

Text S1, Figure S1-S4, and Table S1-S5

451 REFERENCES

452 (1) Yoon, S. W.; Chung, S. W.; Oh, D. G.; Lee, J. W. Monitoring of Non-Point Source
453 Pollutants Load from a Mixed Forest Land Use. *J. Environ. Sci.* **2010**, *22* (6), 801–
454 805.

455 (2) Dove, A.; Chapra, S. C. Long-Term Trends of Nutrients and Trophic Response
456 Variables for the Great Lakes. *Limnol. Oceanogr.* **2015**, *60* (2), 696–721.

457 (3) Boesch, D. F.; Brinsfield, R. B.; Magnien, R. E. Chesapeake Bay Eutrophication:
458 Scientific Understanding, Ecosystem Restoration, and Challenges for Agriculture. *J.*
459 *Environ. Qual.* **2001**, *30* (2), 303–320.

460 (4) Aciego, S. M.; Riebe, C. S.; Hart, S. C.; Blakowski, M. A.; Carey, C. J.; Aarons, S.
461 M.; Dove, N. C.; Botthoff, J. K.; Sims, K. W. W.; Aronson, E. L. Dust Outpaces
462 Bedrock in Nutrient Supply to Montane Forest Ecosystems. *Nat. Commun.* **2017**, *8*, 1–
463 10.

464 (5) Kagatsume, T. Water Conservation Policy of Shiga Prefectural Government. In *Lake*
465 *Biwa: Interactions between Nature and People*; Kawanabe, H., Nishino, M., Maehata,
466 M., Eds.; Springer Netherlands: Dordrecht, 2012; pp 423–427.

(6) Tonderski, K.; Andersson, L.; Lindström, G.; St Cyr, R.; Schönberg, R.; Taubald, H. Assessing the Use of $\delta^{18}O$ in Phosphate as a Tracer for Catchment Phosphorus Sources. *Sci. Total Environ.* **2017**, *607–608*, 1–10.

(7) Paytan, A.; McLaughlin, K. Tracing the Sources and Biogeochemical Cycling of Phosphorus in Aquatic Systems Using Isotopes of Oxygen in Phosphate. In *Handbook of Environmental Isotope Geochemistry*; Baskaran, M., Ed.; Springer Berlin Heidelberg: Berlin, Heidelberg, 2012; Vol. I, pp 419–436.

(8) Tamburini, F.; Pfahler, V.; von Sperber, C.; Frossard, E.; Bernasconi, S. M. Oxygen Isotopes for Unraveling Phosphorus Transformations in the Soil–Plant System: A Review. *Soil Sci. Soc. Am. J.* **2014**, *78*, 38–46.

(9) Davies, C. L.; Surridge, B. W. J.; Gooddy, D. C. Phosphate Oxygen Isotopes within Aquatic Ecosystems: Global Data Synthesis and Future Research Priorities. *Sci. Total Environ.* **2014**, *496*, 563–575.

(10) McLaughlin, K.; Young, M. .; Paytan, A.; Kendall, C. The Oxygen Isotopic Composition of Phosphate: A Tracer for Phosphate Sources and Cycling. In *Application of Isotope Techniques for Assessing Nutrient Dynamics in River Basins*; 2013; pp 93–110.

484 (11) Liang, Y.; Blake, R. E. Oxygen Isotope Signature of Pi Regeneration from Organic
485 Compounds by Phosphomonoesterases and Photooxidation. *Geochim. Cosmochim.*
486 *Acta* **2006**, *70* (15), 3957–3969.

487 (12) Liang, Y.; Blake, R. E. Oxygen Isotope Composition of Phosphate in Organic
488 Compounds: Isotope Effects of Extraction Methods. *Org. Geochem.* **2006**, *37* (10),
489 1263–1277.

490 (13) Liang, Y.; Blake, R. E. Compound- and Enzyme-Specific Phosphodiester Hydrolysis
491 Mechanisms Revealed by $\delta^{18}O$ of Dissolved Inorganic Phosphate: Implications for
492 Marine P Cycling. *Geochim. Cosmochim. Acta* **2009**, *73* (13), 3782–3794.

493 (14) Longinelli, A.; Nuti, S. Revised Phosphate-Water Isotopic Temperature Scale. *Earth*
494 *Planet. Sci. Lett.* **1973**, *19* (3), 373–376.

495 (15) Chang, S. J.; Blake, R. E. Precise Calibration of Equilibrium Oxygen Isotope
496 Fractionations between Dissolved Phosphate and Water from 3 to 37°C. *Geochim.*
497 *Cosmochim. Acta* **2015**, *150*, 314–329.

498 (16) Blake, R. E.; O'Neil, J. R.; Surkov, A. V. Biogeochemical Cycling of Phosphorus:
499 Insights from Oxygen Isotope Effects of Phosphoenzymes. *Am. J. Sci.* **2005**, *305* (6–
500 8), 596–620.

(17) Granger, S. J.; Heaton, T. H. E.; Pfahler, V.; Blackwell, M. S. A.; Yuan, H.; Collins, A. L. The Oxygen Isotopic Composition of Phosphate in River Water and Its Potential Sources in the Upper River Taw Catchment, UK. *Sci. Total Environ.* **2017**, *574*, 680–690.

(18) Gooddy, D. C.; Lapworth, D. J.; Bennett, S. A.; Heaton, T. H. E.; Williams, P. J.; Surridge, B. W. J. A Multi-Stable Isotope Framework to Understand Eutrophication in Aquatic Ecosystems. *Water Res.* **2016**, *88*, 623–633.

(19) Chiara, P.; Tamburini, F.; Gruau, G.; Ferhi, A.; Trevisan, D.; Dorioz, J.-M. Tracing the Sources and Cycling of Phosphorus in River Sediments Using Oxygen Isotopes: Methodological Adaptations and First Results from a Case Study in France. *Water Res.* **2017**, *111*, 346–356.

(20) McLaughlin, K.; Cade-Menun, B. J.; Paytan, A. The Oxygen Isotopic Composition of Phosphate in Elkhorn Slough, California: A Tracer for Phosphate Sources. *Estuar. Coast. Shelf Sci.* **2006**, *70* (3), 499–506.

(21) McLaughlin, K.; Kendall, C.; Silva, S. R.; Young, M.; Paytan, A. Phosphate Oxygen Isotope Ratios as a Tracer for Sources and Cycling of Phosphate in North San Francisco Bay, California. *J. Geophys. Res. Biogeosciences* **2006**, *111*, 1–12.

518 (22) Riley, W. D.; Potter, E. C. E.; Biggs, J.; Collins, A. L.; Jarvie, H. P.; Jones, J. I.; Kelly-
519 Quinn, M.; Ormerod, S. J.; Sear, D. A.; Wilby, R. L.; et al. Small Water Bodies in
520 Great Britain and Ireland: Ecosystem Function, Human-Generated Degradation, and
521 Options for Restorative Action. *Sci. Total Environ.* **2018**, *645*, 1598–1616.

522 (23) Li, X.; Wang, Y.; Stern, J.; Gu, B. Isotopic Evidence for the Source and Fate of
523 Phosphorus in Everglades Wetland Ecosystems. *Appl. Geochemistry* **2011**, *26* (5),
524 688–695.

525 (24) Allen, S. T.; Kirchner, J. W.; Goldsmith, G. R. Predicting Spatial Patterns in
526 Precipitation Isotope (δ^2H and $\delta^{18}O$) Seasonality Using Sinusoidal Isoscapes. *Geophys.*
527 *Res. Lett.* **2018**, 4859–4868.

528 (25) Kendall, C.; Coplen, T. B. Distribution of Oxygen-18 and Deuteriun in River Waters
529 across the United States. *Hydrol. Process.* **2001**, *15* (7), 1363–1393.

530 (26) Bowen, G. J. Isoscapes: Spatial Pattern in Isotopic Biogeochemistry. *Annu. Rev. Earth*
531 *Planet. Sci.* **2010**, *38* (1), 161–187.

532 (27) Shiga Prefecture Department of Lake Biwa and the Environment. *Sewage Work of*
533 *Shiga Prefecture*; 2017.

534 (28) Lake Biwa Environmental Reseach Institute. *Simulation for Future Water Quality*
535 *Prediction Related to "7th Phase of Lake Water Quality Conservation Plan";* 2018.

536 (29) Angert, A.; Weiner, T.; Mazeh, S.; Sternberg, M. Soil Phosphate Stable Oxygen
537 Isotopes across Rainfall and Bedrock Gradients. *Environ. Sci. Technol.* **2012**, *46* (4),
538 2156–2162.

539 31) Hedley, M. J.; Stewart, J. W. B.; Chauhan, B. S. Changes in Inorganic and Organic
540 Soil Phosphorus Fractions Induced by Cultivation Practices and by Laboratory
541 Incubations1. *Soil Sci. Soc. Am. J.* **1982**, *46* (5), 970.

542 (32) Turner, B. L.; Haygarth, P. M. Changes in Bicarbonate-Extractable Inorganic and
543 Organic Phosphorus by Drying Pasture Soils. *Soil Sci. Soc. Am. J.* **2003**, *67* (1), 344–
544 350.

545 (33) Jiang, Z. H.; Zhang, H.; Jaisi, D. P.; Blake, R. E.; Zheng, A. R.; Chen, M.; Zhang, X.
546 G.; Peng, A. G.; Lei, X. T.; Kang, K. Q.; et al. The Effect of Sample Treatments on the
547 Oxygen Isotopic Composition of Phosphate Pools in Soils. *Chem. Geol.* **2017**, *474*
548 (May), 9–16.

549 (34) Murphy, J.; Riley, J. P. A Modified Single Solution Method for the Determination of
550 Phosphate in Natural Waters. *Anal. Chim. Acta* **1962**, *27*, 31–36.

(35) Mellett, T.; Selvin, C.; Defforey, D.; Roberts, K.; Lecher, A. L.; Dennis, K.; Gutknecht, J.; Field, C.; Paytan, A. Assessing Cumulative Effects of Climate Change Manipulations on Phosphorus Limitation in a Californian Grassland. *Environ. Sci. Technol.* **2018**, *52* (1), 98–106.

(36) Hill, W. R.; Mulholland, P. J.; Marzolf, E. R. Stream Ecosystem Responses to Forest Leaf Emergence in Spring. *Ecology* **2001**, *82* (8), 2306–2319.

(37) R Core Team: A Language and Environment for Statistical Computing. R Foundation for Statistical Computing: Vienna, Austria 2018.

(38) Karl, D. M.; Tien, G. MAGIC: A Sensitive and Precise Method for Measuring Dissolved Phosphorus in Aquatic Environments. *Limnol. Oceanogr.* **1992**, *37* (1), 105–116.

(39) Maruo, M.; Ishimaru, M.; Azumi, Y.; Kawasumi, Y.; Nagafuchi, O.; Obata, H. Comparison of Soluble Reactive Phosphorus and Orthophosphate Concentrations in River Waters. *Limnology* **2016**, *17* (1), 7–12.

(40) Young, M. B.; McLaughlin, K.; Kendall, C.; Stringfellow, W.; Rollog, M.; Elsbury, K.; Donald, E.; Paytan, A. Characterizing the Oxygen Isotopic Composition of

Phosphate Sources to Aquatic Ecosystems. *Environ. Sci. Technol.* **2009**, *43* (14), 5190–5196.

(41) Hoellein, T. J.; Tank, J. L.; Rosi-Marshall, E. J.; Entrekin, S. A.; Lamberti, G. A. Controls on Spatial and Temporal Variation of Nutrient Uptake in Three Michigan Headwater Streams. *Limnol. Oceanogr.* **2007**, *52* (5), 1964–1977.

(42) Burmann, F.; Keim, M. F.; Oelmann, Y.; Teiber, H.; Marks, M. A. W.; Markl, G. The Source of Phosphate in the Oxidation Zone of Ore Deposits: Evidence from Oxygen Isotope Compositions of Pyromorphite. *Geochim. Cosmochim. Acta* **2013**, *123*, 427–439.

(43) Markel, D.; Kolodny, Y.; Luz, B.; Nishri, A. Phosphorus Cycling and Phosphorus Sources in Lake Kinneret: Traving by Oxygen Isotopes in Phosphate. *Isr. J. Earth Sci.* **1994**, *43*, 165–178.

(44) Blake, R. E.; Chang, S. J.; Lepland, A. Phosphate Oxygen Isotopic Evidence for a Temperate and Biologically Active Archaean Ocean. *Nature* **2010**, *464* (7291), 1029–1032.

582 (45) Kolodny, Y.; Luz, B.; Navon, O. Oxygen Isotope Variations in Phosphate of Biogenic
583 Apatites, I. Fish Bone Apatite—rechecking the Rules of the Game. *Earth Planet. Sci.*
584 *Lett.* **1983**, *64* (3), 398–404.

585 (46) Morisada, K.; Ono, K.; Kanomata, H. Organic Carbon Stock in Forest Soils in Japan.
586 *Geoderma* **2004**, *119* (1–2), 21–32.

587 (47) Tamburini, F.; Bernasconi, S. M.; Angert, A.; Weiner, T.; Frossard, E. A Method for
588 the Analysis of the $\delta^{18}O$ of Inorganic Phosphate Extracted from Soils with HCl. *Eur. J.*
589 *Soil Sci.* **2010**, *61* (6), 1025–1032.

590 (48) Zohar, I.; Shaviv, A.; Klass, T.; Roberts, K.; Paytan, A. Method for the Analysis of
591 Oxygen Isotopic Composition of Soil Phosphate Fractions. *Environ. Sci. Technol.*
592 **2010**, *44* (19), 7583–7588.

593 (49) Tamburini, F.; Pfahler, V.; Bünemann, E. K.; Guelland, K.; Bernasconi, S. M.;
594 Frossard, E. Oxygen Isotopes Unravel the Role of Microorganisms in Phosphate
595 Cycling in Soils. *Environ. Sci. Technol.* **2012**, *46* (11), 5956–5962.

596 (50) Roberts, K.; Defforey, D.; Turner, B. L.; Condron, L. M.; Peek, S.; Silva, S.; Kendall,
597 C.; Paytan, A. Oxygen Isotopes of Phosphate and Soil Phosphorus Cycling across a

598 6500year Chronosequence under Lowland Temperate Rainforest. *Geoderma* **2015**,
599 *257–258*, 14–21.

600 (51) Helfenstein, J.; Tamburini, F.; von Sperber, C.; Massey, M. S.; Pistocchi, C.;
601 Chadwick, O. A.; Vitousek, P. M.; Kretzschmar, R.; Frossard, E. Combining
602 Spectroscopic and Isotopic Techniques Gives a Dynamic View of Phosphorus Cycling
603 in Soil. *Nat. Commun.* **2018**, *9* (1), 1–9.

604 (52) Pfahler, V.; Tamburini, F.; Bernasconi, S. M.; Frossard, E. A Dual Isotopic Approach
605 Using Radioactive Phosphorus and the Isotopic Composition of Oxygen Associated to
606 Phosphorus to Understand Plant Reaction to a Change in P Nutrition. *Plant Methods*
607 **2017**, *13* (1), 1–12.

608 (53) Gruau, G.; Legeas, M.; Riou, C.; Gallacier, E.; Martineau, F.; Hénin, O. The Oxygen
609 Isotope Composition of Dissolved Anthropogenic Phosphates: A New Tool for
610 Eutrophication Research? *Water Res.* **2005**, *39* (1), 232–238.

611 (54) Zohar, I.; Shaviv, A.; Young, M.; Kendall, C.; Silva, S.; Paytan, A. Phosphorus
612 Dynamics in Soils Irrigated with Reclaimed Waste Water or Fresh Water - A Study
613 Using Oxygen Isotopic Composition of Phosphate. *Geoderma* **2010**, *159* (1–2), 109–
614 121.

615 (55) Gross, A.; Angert, A. What Processes Control the Oxygen Isotopes of Soil Bio-
616 Available Phosphate? *Geochim. Cosmochim. Acta* **2015**, *159*, 100–111.

617

618

619 FIGURE AND TABLE CAPTIONS

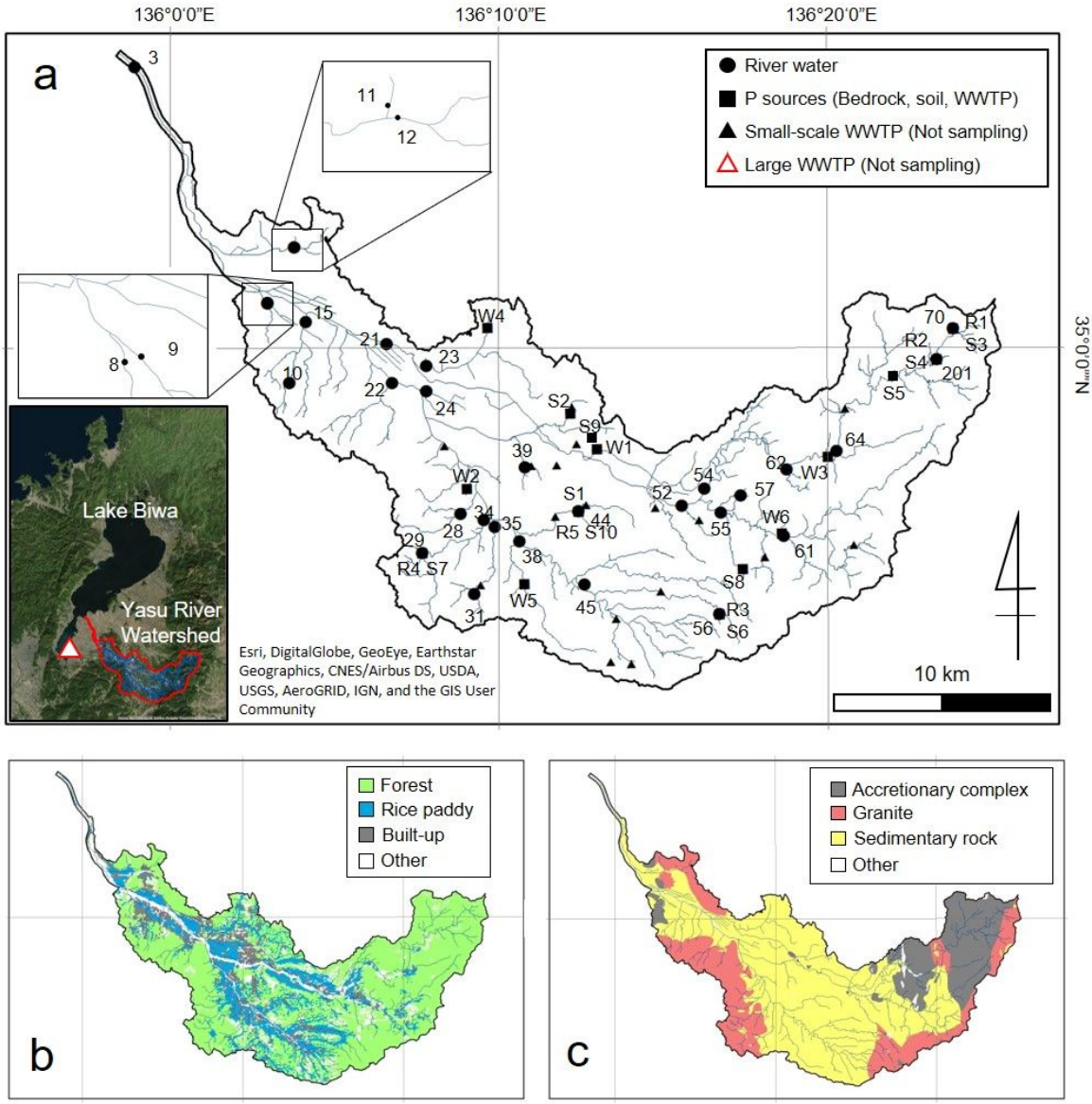

620

621 **Figure 1.** (a) Map of sampling sites for river waters (circles) and potential P sources (squares),

622 and locations of large (open red triangle in small window representing Lake Biwa) and small-

623 scale (closed triangles) wastewater treatment plants (WWTPs) in the catchment of the Yasu

624 River tributary to Lake Biwa in Shiga, Japan. (b) GIS map of land use. (c) GIS map of

625 geological properties. See Table S1 for site IDs and GIS data, and see Tables S2–S4 for
626 abbreviations of sample types.

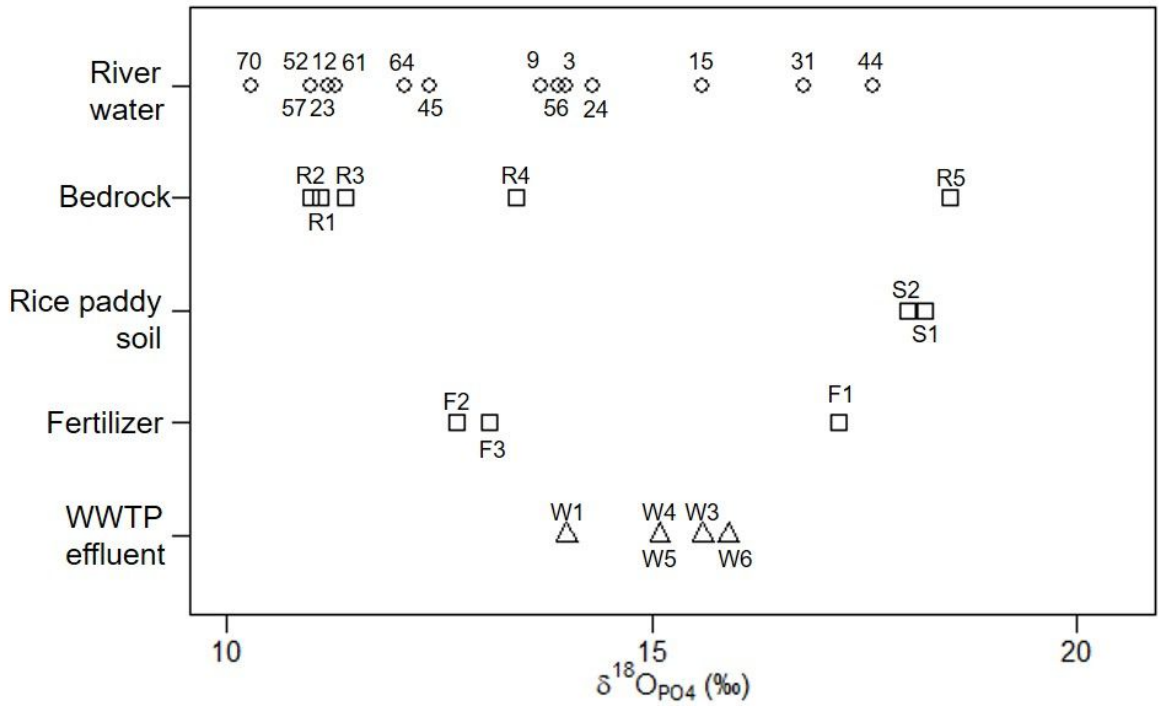

627

628 **Figure 2.** $\delta^{18}O_{PO4}$ values in Yasu River water and P source samples collected within Yasu

629 River Watershed, including bedrocks, rice paddy soils, fertilizers and wastewater treatment

630 plant (WWTP) effluents. Numbers on symbols refer to sampling sites as shown in Fig. 1.

631

632

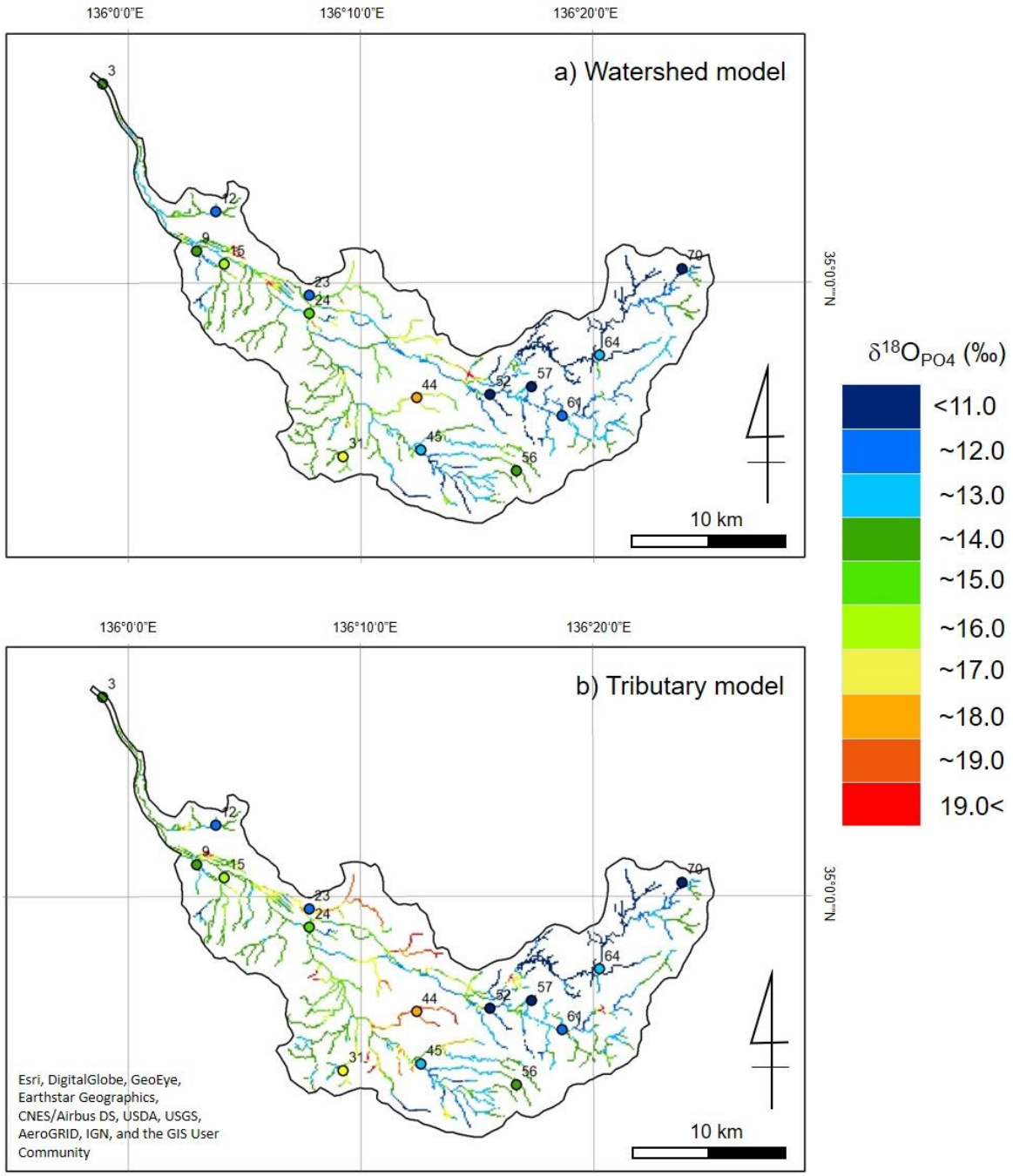

633

634 **Figure 3.** Isoscapes of river water $\delta^{18}O_{PO4}$ based on (a) watershed model and (b) tributary

635 model. Colored circles and numbers refer to the observed $\delta^{18}O_{PO4}$ values in the river water and

636 sampling sites. See text for details of the two models.

637 **Table 1.** Multiple-regression statistics for the best fits of the watershed and tributary models

638 based on AIC. VIF = variance inflation factor. See text for details of the two models.

	Variables	Coefficient	S.E.	*p*	VIF	R^2
Watershed model	Intercept	10.0	1.40	0.001	-	0.69
	Accretionary complex	-3.18	1.36	0.04	1.5	
	Forest	3.40	1.77	0.08	2.0	
	Rice paddy	11.1	3.17	0.01	1.7	
Tributary model	Intercept	10.5	0.68	0.001	-	0.96
	Accretionary complex	-11.2	1.75	0.001	8.4	
	Granite	-8.05	1.76	0.01	9.9	
	Forest	11.3	1.81	0.002	7.8	
	Rice paddy	5.60	2.06	0.04	2.7	

639

640 TOC art

641